Journal of Organometallic Chemistry, 394 (1990) 417–432
Elsevier Sequoia S.A., Lausanne
JOM 20918

A phosphorus–carbon bond cleavage reaction of coordinated trimethylphosphine in $(PMe_3)_4Ru(OC_6H_4Me)_2$ *

John F. Hartwig, Robert G. Bergman and Richard A. Andersen
Department of Chemistry, University of California, Berkeley, CA 94720 (U.S.A.)
(Received February 13th, 1990)

Abstract

A product resulting from cleavage of the P–C bond in a trimethylphosphine ligand forms upon thermolysis of $(PMe_3)_4Ru(OC_6H_4Me)_2$ (**1**) or addition of *p*-cresol to the orthometallated complex $(PMe_3)_4Ru(\eta^2\text{-}OC_6H_3Me)$ (**2**). The trimethylphosphine ligand has been transformed to a dimethylarylphosphinite ligand in the product $(PMe_3)_3(\eta^2\text{-}PMe_2OC_6H_3)Ru(OC_6H_4Me)$ (**3**). Although complex **1** exists in equilibrium with complex **2** and free *p*-cresol at 65 °C, kinetic evidence is presented indicating that complex **1** undergoes the P–C cleavage reaction. An X-ray crystal structure analysis was performed on **3**. Crystal data at 25 °C: *a* 11.8875(11), *b* 36.000(4), *c* 14.1207(13) Å, $\beta = 90.428(8)°$, $Z = 8$, D_{calc} 1.33 g/cm^3; space group $P2_1/n$.

Introduction

Phosphines are among the most common ligands in coordination and organometallic chemistry, and metal phosphine complexes are often used as homogeneous catalysts [1]. They are important because of their strong electron-donating properties [2], and in most cases they are inert toward reactions other than addition of their C–H bonds [3]. However, it has been noted that the cleavage of the P–C bond is a possible decomposition route for some catalysts containing aryl phosphine ligands; products resulting from the cleavage of the P–C bond in aryl phosphine ligands have been isolated [4]. In contrast, evidence for cleavage of the P–C bond in trialkylphosphine compounds has been reported in only a few cases [5]. To our knowledge, no product has been isolated in which a coordinated trialkylphosphine has been structurally changed as a result of P–C bond cleavage. We report such a

* This paper is dedicated to Prof. F. Gordon A. Stone on the occasion of his sixty-fifth birthday.

0022-328X/90/$03.50

reaction, in which a trimethylphosphine ligand of $(PMe_3)_4Ru(OAr)_2$ is transformed under mild thermolysis conditions into an orthometallated dimethylarylphosphinite ligand, the result of P–C bond cleavage.

Results and discussion

The aryloxide compound $(PMe_3)_4Ru(OAr)_2$ (**1**) was prepared by the addition of two equivalents of *p*-cresol (*p*-methylphenol) to $(PMe_3)_4Ru(Me)_2$ [6] in toluene to form **1** in 66% isolated yield (Scheme 1). An AA'BB' pattern in the aryl region of the ^1H NMR spectrum of **1** indicates η^1 coordination of the two equivalent *p*-cresolate substituents, and an A_2B_2 pattern in the $^{31}P\{^1H\}$ NMR spectrum indicates that the complex adopts a *cis* geometry.

Addition of one equivalent of *p*-cresol to $(PMe_3)_4Ru(Me)_2$ yielded roughly 50% of **1** and 50% of starting material. However, use of $(PMe_3)_3Ru(\eta^2\text{-}CH_2PMe_2)(Me)$ allowed the selective addition of one equivalent of *p*-cresol to the ruthenium center. This cyclometallated precursor was synthesized in 40% isolated yield by the thermolysis of $(PMe_3)_4Ru(Me)_2$ in hexane followed by sublimation. Addition of one equivalent of *p*-cresol to $(PMe_3)_3Ru(\eta^2\text{-}CH_2PMe_2)(Me)$ at room temperature followed by heating to 85 °C for 3 h did not provide the simple addition product, but yielded methane (identified by ^1H NMR spectroscopy) and the orthometallated cresolate complex $(PMe_3)_4Ru(\eta^2\text{-}OC_6H_3Me)$ (**2**) in 56% isolated yield. The observation of three aryl resonances in the ^1H NMR spectrum of **2** in a 1 : 1 : 1 ratio, as well as an A_2BC pattern in its $^{31}P\{^1H\}$ NMR spectrum, indicated orthometallation of the aryl ring had occurred.

Thermolysis of **1** in benzene for 8 h at 85 °C or 70 h at 65 °C also produced methane (identified by ^1H NMR spectroscopy) and complex **3**, the product of P–C bond cleavage, in quantitative yield by ^1H NMR spectroscopy and 34% isolated yield, as shown in Scheme 2. The $^{31}P\{^1H\}$ NMR spectrum of **3** contained two resonances in the chemical shift range associated with PMe_3 groups coordinated to ruthenium [7] and a deshielded resonance at 172 ppm. The latter resonance is in the range found for coordinated phosphite ligands [8]. The $^{31}P\{^1H\}$ NMR spectrum is

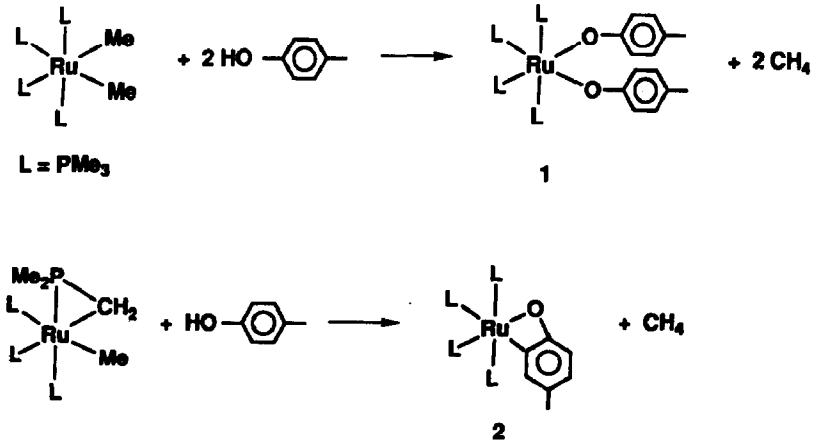

Scheme 1

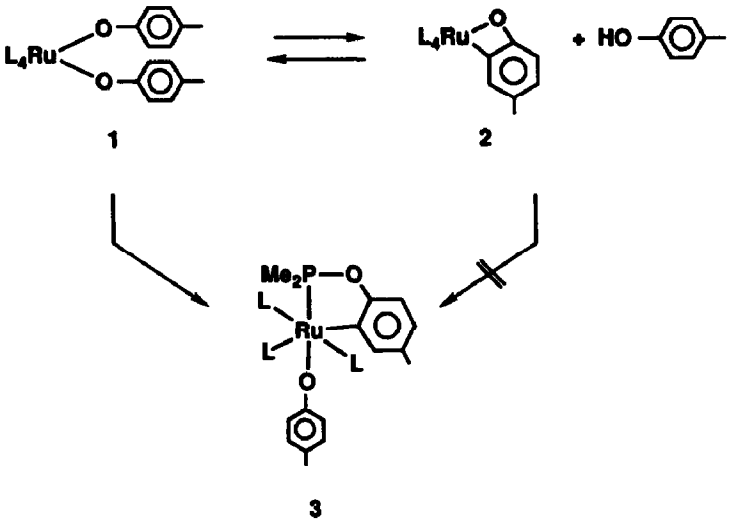

Scheme 2

an example of an A_2BX spin system. The two equivalent phosphorus nuclei appear as a doublet of doublets centered at δ −1.69 with J_{AB} = 24.3 Hz and J_{AX} = 37.2 Hz. The other PMe_3 resonance appears as a doublet of triplets centered at δ −19.2 with J_{AB} = 24.3 Hz and J_{BX} = 9.0 Hz. The X nucleus appears as a doublet of triplets at δ 172.3. The coupling constants are consistent with a geometry in which equivalent phosphines P_A are *trans* to each other and are *cis* to P_B and P_X. The ^1H NMR spectrum shows a phosphine methyl group ratio of 18 : 9 : 6, indicating that one of the phosphines assigned to P_x contains only two methyl substituents. The ^1H NMR spectrum requires the presence of two types of *p*-cresolate ligands, one of which shows an AA'BB' pattern for the ring protons, similar to that found in **1**. The other cresolate shows an ABC_4 pattern for the ring protons similar to those found in **2**, consistent with ring metallation in the *ortho*-position. Two isomers, **A** and **B**, shown in Fig. 1, are consistent with the spectroscopic observations, and we could not distinguish between them spectroscopically, though both contain coordinated dimethylphosphinite ligands of two different types. A few coordinated dialkylphosphinites have been described and their $^{31}P\{^1H\}$ NMR chemical shifts are in the range of δ 140 to 160 [9].

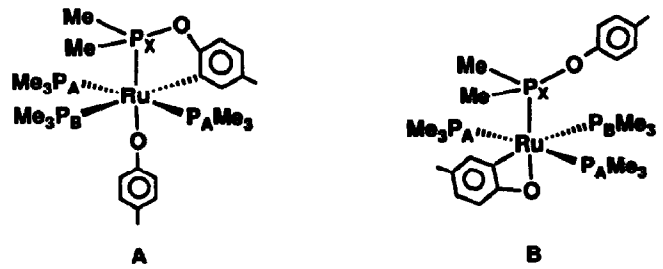

Fig. 1. Two structures consistent with spectroscopic data for **3**.

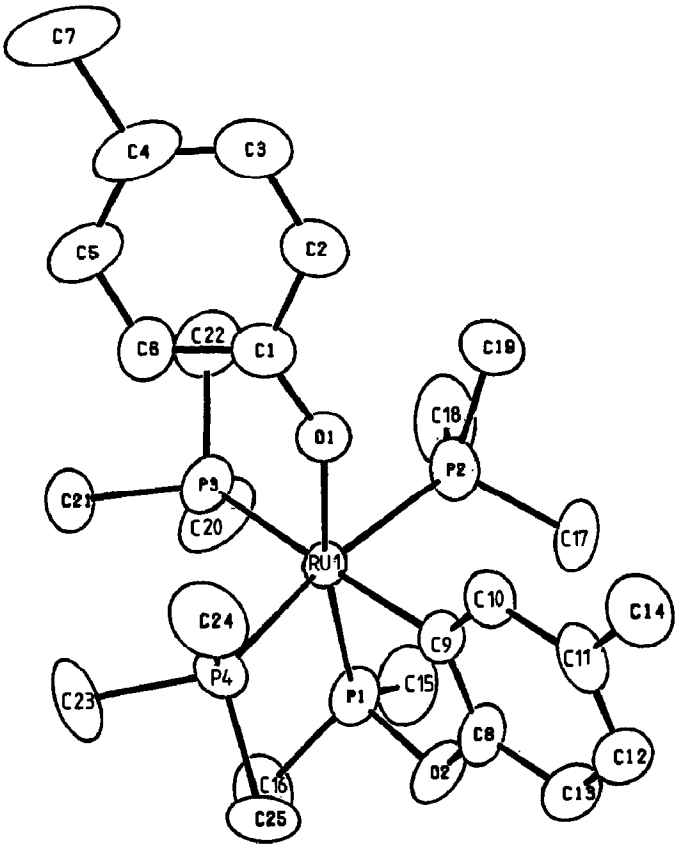

Fig. 2. ORTEP diagram of complex 3. The hydrogen atoms are omitted for clarity.

X-ray crystallography shows that **A** is the correct structure. Compound **3** crystallized from a toluene/pentane solution at $-40\,^{\circ}C$. The structure was solved by Patterson methods and refined via standard least-squares and Fourier techniques. The space group is $P2_1/n$ with two crystallographically independent but chemically identical molecules in the asymmetric unit. The structure contained no abnormally short intermolecular distances. An ORTEP diagram of one of the two molecules is shown in Fig. 2. Intramolecular bond distances and angles for this molecule are given in Tables 1 and 2, and the positional and thermal parameters are given in Tables 3 and 4. The geometry of the complex is based upon six-coordinate Ru(II) with two mutually *trans* PMe_3 ligands, a PMe_3 *trans* to the metallated aryl ring of the phosphinite ligand, and an η^1-cresolate ligand *trans* to the phosphorus of the phosphinite ligand.

The Ru–P(2,4) distances of 2.357(2) Å and 2.366(2) Å are in the range found in related alkylphosphine derivatives of Ru(II) in six coordination [7,10*]. The lengths of the mutually *trans* phosphine–ruthenium bonds range from 2.2 to 2.4 Å. The Ru–P(3) distance of 2.381(2) Å is in the region found for Ru–P (ca. 2.32 Å) *trans* to a carbon ligand [7a,c,g]. The Ru–P(1) bond length of 2.199(2) Å is the shortest Ru–P distance in the structure. Since values for metal–dialkylphosphinite bonds are

* Reference number with asterisk indicates a note in the list of references.

Table 1

Crystallographic data for complex 3; empirical formula: $C_{25}H_{46}O_2P_4Ru$

a. Crystal parameters at $T = 25°C$	
a 11.8875(11) Å	Space group: $P2_1/n$
b 36.000(4) Å	Formula weight = 603.6 amu
c 14.1207(13) Å	$Z = 8$
$\alpha = 90.0°$	d(calc) 1.33 g cm^{-3}
$\beta = 90.428(8)°$	
$\gamma = 90.0°$	μ(calc) 7.4 cm^{-1}
V 6042.7(18) Å^3	
Size: 0.10×0.20×0.29 mm	

b. Data measurement parameters [8]	
Radiation: Mo-K_α ($\lambda = 0.71073$ Å)	
Monochromator: highly oriented graphite ($2\|\| = 12.2$)	
Detector: crystal scintillation counter, with PHA	
Reflections measured: $+H, +K, \pm -L$	
2θ range: 3– > 45 deg	Scan type: θ–2θ
Scan width: $\Delta\theta = 0.60 + 0.60 \tan\theta$	
Scan speed: 0.72– > 6.70 (θ, deg/min)	
Background: measured over 0.25 $\Delta\theta$ added to each end of the scan.	
Vertical aperture = 3.0 mm	Horizontal aperture = $2.0 + 1.6 \tan\theta$ mm
No. of reflections collected: 8048	
No. of unique reflections: 7642	

Table 2

Intramolecular distances

Atom 1	Atom 2	Distance	Atom 1	Atom 2	Distance
Ru1	P1	2.199(2)	O1	C1	1.327(10)
Ru1	P2	2.357(2)	C1	C2	1.419(13)
Ru1	P3	2.381(2)	C1	C6	1.439(10)
Ru1	P4	2.366(1)	C2	C3	1.401(19)
Ru1	O1	2.161(4)	C3	C4	1.389(15)
Ru1	C9	2.092(8)	C4	C5	1.373(13)
			C4	C7	1.576(16)
P1	C15	1.811(7)	C5	C6	1.384(12)
P1	C16	1.861(7)			
P1	O2	1.667(4)	O2	C8	1.371(11)
P2	C17	1.857(7)	C8	C9	1.426(12)
P2	C18	1.868(7)	C8	C13	1.421(9)
P2	C19	1.856(7)	C9	C10	1.376(12)
P3	C20	1.851(8)	C10	C11	1.435(10)
P3	C21	1.836(7)	C11	C12	1.421(18)
P3	C22	1.839(7)	C11	C14	1.527(12)
P4	C23	1.865(6)	C12	C13	1.380(18)
P4	C24	1.825(6)			
P4	C25	1.859(6)			

Table 3

Intramolecular angles

Atom 1	Atom2	Atom 3	Angle	Atom 1	Atom 2	Atom 3	Angle
P1	Ru1	P2	92.67(7)	Ru1	P1	O2	106.62(16)
P1	Ru1	P3	97.91(6)	Ru1	P1	C15	125.7(3)
P1	Ru1	P4	92.09(6)	Ru1	P1	C16	122.81(23)
P1	Ru1	O1	167.00(11)	Ru1	P2	C17	115.90(23)
P1	Ru1	C9	81.6(3)	Ru1	P2	C18	122.7(3)
P2	Ru1	P3	93.34(6)	Ru1	P2	C19	113.52(22)
P2	Ru1	P4	162.59(6)	Ru1	P3	C20	117.2(3)
P2	Ru1	O1	83.98(11)	Ru1	P3	C21	123.47(25)
P2	Ru1	C9	83.61(16)	Ru1	P3	C22	116.4(3)
P3	Ru1	P4	102.58(6)	Ru1	P4	C23	123.46(23)
P3	Ru1	O1	94.83(11)	Ru1	P4	C24	113.27(22)
P3	Ru1	C9	176.88(17)	Ru1	P4	C25	118.59(24)
P4	Ru1	O1	87.65(11)	C15	P1	O2	99.2(3)
P4	Ru1	C9	80.53(16)	C16	P1	O2	100.9(3)
O1	Ru1	C9	85.5(3)	C15	P1	C16	97.0(3)
				C17	P2	C18	99.1(3)
				C17	P2	C19	100.2(3)
				C18	P2	C19	102.0(4)
				C20	P3	C21	97.3(4)
				C20	P3	C22	100.4(4)
				C21	P3	C22	97.7(3)
				C23	P4	C24	100.5(3)
				C23	p4	C25	97.6(3)
				C24	P4	C25	99.3(3)

not known, we must use other comparisons to see if this value is unusual, that is, if $M-P(OR)_x(R)_{3-x}$ distances are typically shorter than those for $M-PR_3$. In structurally similar d^6 compounds, $(CO)_5CrP(OPh)_3$ and $(CO)_5CrPPh_3$ [11], $BrMn(CO)_3(P(OMe)_2Ph)_2$ [12] and $BrMn(CO)(PPh_3)$ [13], and in *trans*-$[(PhO)_3P][Ph_3P]Cr(CO)_4$ [14], the metal–phosphite or –phosphonite bond lengths are shorter than the metal–phosphine bond lengths by 0.1 to 0.16 Å. The difference is usually rationalized in terms of the stronger π-accepting character of the phosphite and phosphonite ligands. Thus, the shorter distance for the ruthenium–dimethylphosphinite bond seems to agree with previous results. The π-accepting nature of the $Me_2P(OAr)$ ligand and the π-donating ability of the aryloxide ligand which is located *trans* to it may lead to the shorter Ru–P(3) distance.

The P–C cleavage product **3** was also obtained by the addition of *p*-cresol to the orthometallated cresolate complex **2** followed by heating under the same conditions as the thermolysis of **1**. Moreover, when the thermolysis of **1** or **2** and cresol was stopped before completion (16 h at 65 °C), a mixture of starting complex **1**, orthometallated cresolate complex **2**, and P–C cleaved product **3** was observed as shown in Scheme 2). From these data it cannot be determined if **1** or **2** gives rise to the P–C cleavage reaction, since these two complexes interconvert at a rate which is faster than the formation of **3**. Addition of phenol, rather than *p*-cresol, to **2** yielded a mixture of P–C cleaved products due presumably to rapid scrambling of the aryloxide ligands, and provided no insight into this problem.

Table 4

Positional parameters and their estimated standard deviations

Atom	x	y	z	B (Å^2)
Ru1	0.25495(6)	−0.03622(2)	0.25611(5)	2.61(1)
Ru2	0.23155(7)	0.20588(2)	0.03895(5)	3.15(2)
P1	0.1849(2)	−0.09212(8)	0.2339(2)	3.96(6)
P2	0.2157(2)	−0.03731(9)	0.4194(2)	4.28(7)
P3	0.4464(2)	−0.05375(9)	0.2791(2)	4.23(7)
P4	0.2472(2)	−0.02275(7)	0.0922(2)	3.20(6)
P5	0.1511(3)	0.15252(8)	0.0737(2)	4.71(7)
P6	0.1846(3)	0.20181(9)	−0.1232(2)	4.93(7)
P7	0.4176(3)	0.18373(9)	0.0163(2)	4.93(8)
P8	0.2366(3)	0.22397(9)	0.2005(2)	4.86(7)
O1	0.2842(5)	0.0223(2)	0.2802(4)	3.7(2)
O2	0.0476(5)	−0.0867(2)	0.2136(5)	4.8(2)
O3	0.2721(6)	0.2625(2)	0.0043(5)	4.3(2)
O4	0.0172(7)	0.1611(2)	0.0949(7)	4.0(3)
C1	0.3666(8)	0.0472(3)	0.2807(7)	4.0(2)
C2	0.3615(9)	0.0771(3)	0.3459(7)	4.5(3)
C3	0.4469(9)	0.1039(3)	0.3508(8)	4.8(3)
C4	0.5394(9)	0.1014(3)	0.2916(8)	5.5(3)
C5	0.5460(9)	0.0730(3)	0.2268(8)	5.0(3)
C6	0.4636(9)	0.0460(3)	0.2205(8)	4.5(3)
C7	0.636(1)	0.1315(4)	0.297(1)	7.7(3)
C8	0.0083(8)	−0.0512(3)	0.2258(7)	4.1(2)
C9	0.0852(7)	−0.0216(3)	0.2436(6)	3.1(2)
C10	0.0402(8)	0.0135(3)	0.2525(6)	3.5(2)
C11	−0.0780(8)	0.0208(3)	0.2435(7)	4.2(2)
C12	−0.1518(8)	−0.0098(3)	0.2296(7)	4.4(3)
C13	−0.1098(8)	−0.0454(3)	0.2205(7)	4.7(3)
C14	−0.1227(9)	0.0605(3)	0.2508(8)	5.2(3)
C15	0.179(1)	−0.1286(3)	0.3220(9)	6.2(3)
C16	0.225(1)	−0.1221(3)	0.1320(9)	5.9(3)
C17	0.0698(9)	−0.0504(4)	0.4518(8)	5.9(3)
C18	0.294(1)	−0.0673(4)	0.5051(8)	7.7(4)
C19	0.225(1)	0.0090(4)	0.4767(7)	5.7(3)
C20	0.474(1)	−0.1015(4)	0.322(1)	7.2(4)
C21	0.5513(9)	−0.0533(4)	0.1843(8)	5.5(3)
C22	0.527(1)	−0.0268(4)	0.3670(9)	6.8(4)
C23	0.359(1)	−0.0366(4)	0.0073(7)	6.0(3)
C24	0.237(1)	0.0268(3)	0.0668(8)	5.3(3)
C25	0.124(1)	−0.0395(4)	0.0221(8)	6.0(3)
C26	0.3577(9)	0.2868(3)	0.0027(7)	4.0(2)
C27	0.4541(9)	0.2835(3)	0.0580(7)	4.6(3)
C28	0.538(1)	0.3106(3)	0.0491(9)	5.7(3)
C29	0.530(1)	0.3413(3)	−0.0073(9)	6.0(3)
C30	0.4321(9)	0.3436(3)	−0.0639(8)	5.4(3)
C31	0.3485(9)	0.3169(3)	−0.0603(8)	5.1(3)
C32	0.625(1)	0.3697(4)	−0.011(1)	8.1(4)
C33	−0.015(1)	0.1975(4)	0.079(1)	6.5(3)
C34	0.0646(8)	0.2246(3)	0.0537(8)	4.5(3)
C35	0.0269(9)	0.2607(3)	0.0386(7)	4.8(3)
C36	−0.089(1)	0.2701(4)	0.0491(8)	6.2(3)
C37	−0.167(1)	0.2410(4)	0.070(1)	7.8(4)
C38	−0.130(1)	0.2052(4)	0.087(1)	8.3(4)
C39	−0.121(1)	0.3106(4)	0.037(1)	7.8(4)

Table 4 (continued)

Atom	x	y	z	B (Å^2)
C40	0.133(1)	0.1138(3)	−0.0146(9)	6.8(3)
C41	0.192(1)	0.1248(4)	0.1787(9)	6.9(4)
C42	0.246(1)	0.1661(4)	−0.2067(9)	8.4(4)
C43	0.036(1)	0.1938(4)	−0.1534(9)	7.3(4)
C44	0.209(1)	0.2456(4)	−0.1883(8)	8.2(4)
C45	0.431(1)	0.1342(4)	−0.016(1)	7.8(4)
C46	0.497(1)	0.2052(4)	−0.079(1)	7.4(4)
C47	0.525(1)	0.1829(4)	0.110(1)	7.9(4)
C48	0.115(1)	0.2129(4)	0.2737(9)	8.4(4)
C49	0.358(1)	0.2115(4)	0.2781(9)	8.7(4)
C50	0.236(1)	0.2739(3)	0.2163(8)	6.0(3)

The thermal parameter given for anisotropically refined atoms is the isotropic equivalent thermal parameter defined as: $(4/3)\cdot[a^2\cdot\beta(1,1)+b^2\cdot\beta(2,2)+c^2\cdot\beta(3,3)+ab(\cos\gamma)\cdot\beta(1,2)+ac(\cos\beta)\cdot\beta(1,3)+bc(\cos\alpha)\cdot\beta(2,3)]$ where a, b, c are real cell parameters, and $\beta(i,j)$ are anisotropic betas.

Careful monitoring of the reaction by ^{1}H NMR spectroscopy provided evidence that it is the biscresolate complex **1** that gives rise to the P–C cleaved product. The appearance of product was followed at 65 °C for 2.5 half lives using three different NMR tubes: one containing only **1**, one containing equivalent concentrations of **3** and *p*-cresol, and one containing the equilibrium concentrations of all three reactants. Identical linear first-order plots for disappearance of total metal complex vs. time were obtained in all three cases ($k_{obs} = 8.7 \times 10^{-6}$ s^{-1}) for the data points collected after an initial period during which time equilibrium was established (5 h). The data collected over this time were not accurate enough to extract rate constants for the approach to equilibrium, but it was clear that the sample containing only **1** reacted at a faster initial rate than the equilibrium mixture, while the sample containing **2** and *p*-cresol reacted more slowly than the equilibrium mixture and showed an initial induction period as displayed in Fig. 3. In all three cases, the formation of **3** was strongly inhibited by the addition of PMe_3 to the reaction solution. No product was observed after 3 d for the tubes containing added PMe_3,

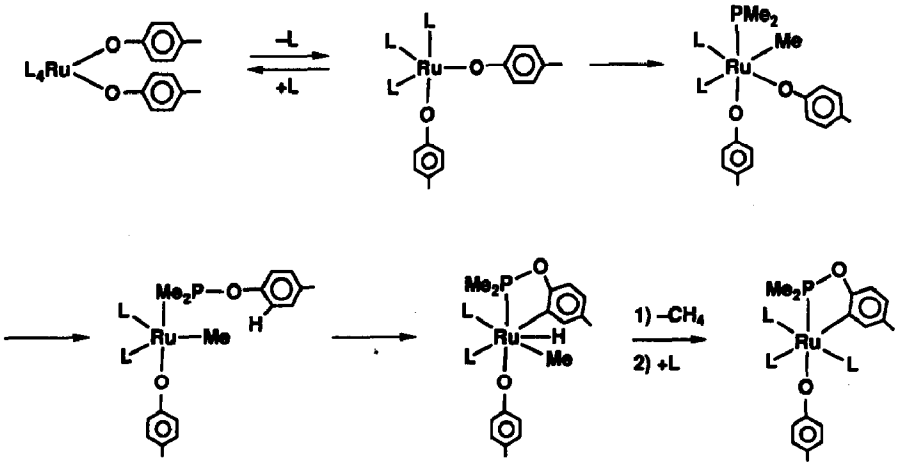

Scheme 3

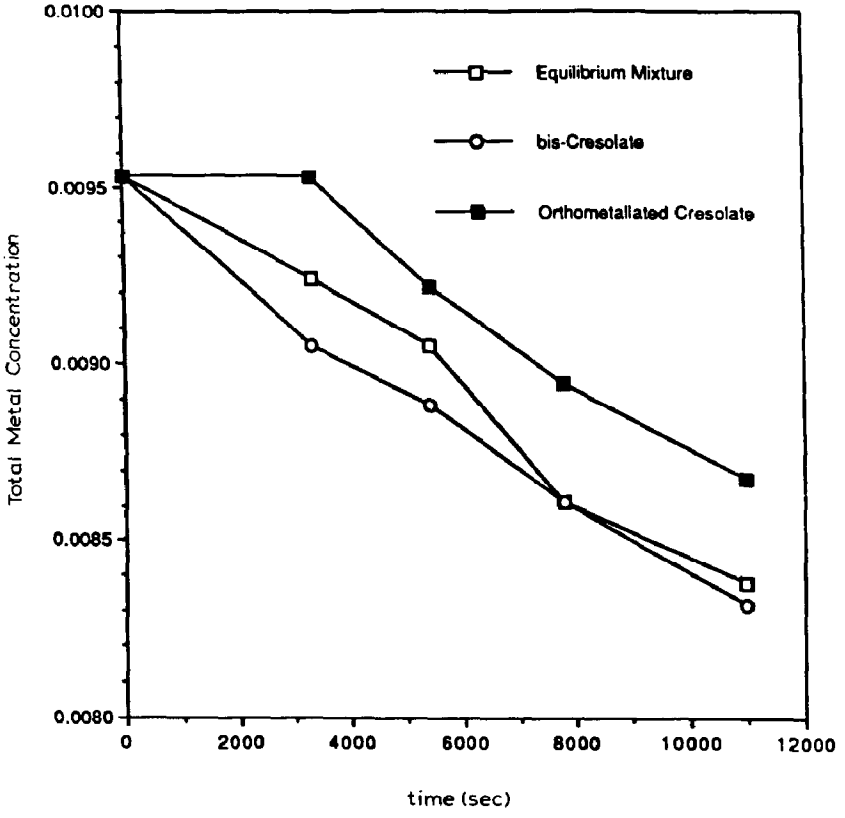

Fig. 3. A comparison of the rate fo formation of **3** from samples containing only biscresolate complex **1**, orthometallated cresolate complex **2** and the equilibrium mixture of the two.

while reaction was complete for the samples containing no added PMe_3. However, the equilibrium was established at roughly the same rate for the tubes containing added phosphine as for those containing no added phosphine. Although we have no direct mechanistic information about the fundamental phosphorus–carbon bond cleavage step, we suggest that dissociation of phosphine precedes oxidative addition of the P–C bond (Scheme 3), as has been proposed [4] for the decomposition of aryl phosphine ligands. Migration of the aryloxide ligand to the phosphido substituent of the intermediate formed by this process followed by orthometallation would form **3**.

Experimental

General

Unless otherwise noted, all manipulations were carried out under an inert atmosphere in a Vacuum Atmosphere 553-2 drybox with attached M6-40-1H Dritrain, or by using standard Schlenk or vacuum line techniques.

^{1}H NMR spectra were obtained on either the 250, 300, 400 or 500 MHz Fourier Transform spectrometers at the University of California, Berkeley (UCB) NMR facility. The 250 and 300 MHz instruments were constructed by Mr Rudi Nunlist and interfaced with either a Nicolet 1180 or 1280 computer. The 400 and 500 MHz

Table 5

^{1}H NMR spectroscopic data [a]

Compound	δ (ppm)	Multiplicity	J(Hz)	Integral	Assignment
$(PMe_3)_3ru(\eta^2\text{-}CH_2PMe_2)Me$	−0.41	dddd	7.7, 7.7, 7.5, 3.6	3	Me
	−0.58	m		1	CH_2PMe_2
	−0.24	m		1	
	1.10	d	5.3	9	PMe_3
	1.21	dd	7.9, 3.3	9	
	1.24	dd	7.0, 1.8,	9	
	1.18	dd	9.0, 5.3	3	CH_2PMe_2
	1.28	dd	8.9, 2.4	3	
$(PMe_3)_4Ru(OC_6H_4Me)_2$ (1)	0.96	d	7.7	18	*cis*-PMe_3
	1.14	N [b]	6.2	19	*trans*-PMe_3
	2.40	s		6	*p*-Me
	7.04	d	8.4	4	aromatic
	7.22	d	8.4	4	
$(PMe_3)_4Ru(\eta^2\text{-}OC_6H_3Me)$ (2)	1.00	d	7.4	9	*cis*-PMe_3
	1.09	d	6.0	9	
	1.15	N	5.8	18	*trans*-PMe_3
	2.58	s		3	*p*-Me
	6.06	d	7.6	1	aromatic
	6.96	d	7.2	1	
	7.30	br, s		1	
$(PMe_3)_3(\eta^2\text{-}PMe_2OC_6H_3)Ru(OC_6H_4Me)$ (3)	0.92	N	6.2	18	*trans*-PMe_3
	1.06	d	5.5	9	*cis*-PMe_3
	1.29	d	6.4	6	Me_2POAr
	2.42	s		3	*p*-Me
	2.43	s		3	
	6.89	d	7.4	2	OC_6H_4Me
	7.04	d	7.8	2	
	6.67	dd	6.4, 2	1	$ArOPMe_2$
	7.04	dd	7.8, 2	1	
	8.10	br, s		1	

[a] C_6D_6 solvent. [b] The value of N refers to the separation between the two outermost lines. See R.K. Harris and R.G. Hayter, Can. J. Chem., 42 (1964) 2282; R.K. Harris, Can. J. Chem., 42 (1964) 2275.

instruments were commercial Bruker AM series spectrometers. ^{1}H NMR spectra were recorded relative to residual protiated solvent. ^{13}C NMR spectra were obtained at either 75.4 or 100.6 MHz on the 300 or 500 MHz instruments, respectively, and chemical shifts were recorded relative to the solvent resonance. NMR data are shown in Tables 5–7; chemical shifts are reported in units of parts per million downfield from tetramethylsilane and all coupling constants are reported in hertz.

IR spectra were obtained on a Perkin-Elmer Model 283 infrared spectrometer or on a Perkin-Elmer Model 1550 or 1750 FT-IR spectrometer using potassium bromide ground pellets. Mass spectroscopic (MS) analyses were obtained at the UCB mass spectrometry facility on AEI MS-12 and Kratos MS-50 mass spectrometers. Elemental analyses were obtained from the UCB Microanalytical Laboratory.

Sealed NMR tubes were prepared by fusing Wilmad 505-PP and 504-PP tubes to ground glass joints which were then attached to a vacuum line with Kontes

Table 6

$^{13}C\{^1H\}$ NMR spectroscopic data

Compound	δ (ppm)	Multiplicity [a]	J(Hz)	Assignment
$(PMe_3)_3Ru(\eta^2\text{-}PMe_2CH_2)Me$ [b]	24.73	dd	18.0, 7.5	PMe_3
	24.57	d	15.4	
	22.10	d	20.1, 2.6	
	15.36	td	9.3, 3.5	PMe_2PCH_2
	5.78	dd	7.7, 6.6	
	−1.27	dq	54.1, 11.7	Me
	−10.57	m		PMe_2PCH_2
$(PMe_3)_4Ru(OC_6H_4Me)_2$ (1) [c]	18.65	t	12.6	*trans*-PMe_3
	22.57	m		*cis*-PMe_3
	20.75	s		*p*-Me
	118.36	s		Aromatic
	120.66	s		
	129.68	s		
	169.41	s		
$(PMe_3)_4Ru(\eta^2\text{-}OC_6H_3Me)$(2) [c]	18.65	td	13.5, 3.0	*trans*-PMe_3
	22.44	dt	18.1, 2.6	*cis*-PMe_3
	25.32	dq	25.0, 3.4	
	21.88	s		*p*-Me
	105.55	s		aromatic
	120.44	s		
	122.00	s		
	137.80	s		
	142.69	dtd	65, 16, 6	
	182.41	s		
$(PMe_3)_3(\eta^2\text{-}PMe_2OC_6H_3)Ru(OC_6H_4Me)$ (3) [c]	18.40	t	13.4	PMe_3 and
	23.89	d	18.1	Me_2POAr
	27.39	d	30	
	20.72	s		*p*-Me
	21.49	s		
	112.86	dd	13, 0.6	aromatic groups
	120.79	s		
	123.51	s		
	126.73	t	2	
	131.48	dd	4.2	
	132.41	s		
	140.61	s		
	162.72	dq	43, 12	
	165.80	dq	11.1, 2.2	
	172.81	d	1.8	

[a] The symbols d and t, when applied to the PMe_3 resonances are observed patterns, not true multiplicity patterns. Accordingly, the values reported as coupling constants for these resonances are the separation between lines and do not necessarily reflect the true coupling constants. [b] C_6D_6. [c] THF-d_8.

stopcocks or, alternatively, the tubes were attached via Cajon adapters directly to Kontes vacuum stopcocks [15]. Known volume bulb vacuum transfers were accomplished with an MKS Baratron attached to a high vacuum line.

Unless otherwise specified, all reagents were purchased from commercial suppliers and used without further purification. PMe_3 (Strem) was dried over NaK or a

Table 7

$^{31}P\{^1H\}$ NMR spectroscopic data [a]

Compound	Spin system	δ (ppm)	J(Hz)
$(PMe_3)_3Ru(\eta^2\text{-}PMe_2CH_2)Me$	ABCD	δ_A 5.76	J_{AB} 0
		δ_B 0.64	J_{AC} 27
		δ_C −7.61	J_{AD} 231
		δ_D 37.93	J_{BC} 24
			J_{BD} 38
			J_{CD} 24
$(PMe_3)_4Ru(OC_6H_4Me)_2$ (1)	A_2B_2	δ_A 14.89	J_{AB} 31.8
		δ_B −0.98	
$(PMe_3)_4Ru(\eta^2\text{-}OC_6H_3Me)$ (2)	A_2BC	δ_A −2.73	J_{AB} 34
		δ_B 15.78	J_{AC} 24
		δ_C −9.31	J_{BC} 17
$(PMe_3)_3(\eta^2\text{-}PMe_2OC_6H_3)Ru(OC_6H_4Me)$ (3)	A_2BC	δ_A −1.69	J_{AX} 37.2
		δ_B −19.24	J_{AB} 24.3
		δ_X 172.29	J_{BX} 9.0

[a] C_6D_6 solvent.

Na mirror and vacuum transferred prior to use. Ferrocene (Aldrich) was sublimed prior to use. *p*-Cresol was dried by refluxing a solution in benzene using a Dean Stark trap followed by distillation under argon.

Pentane and hexane (UV grade, alkene free) were distilled from $LiAlH_4$ under nitrogen. Benzene, toluene, and tetrahydrofuran were distilled from sodium benzophenone ketyl under nitrogen. Dichloromethane was either distilled under N_2 or vacuum transferred form CaH_2. Deuterated solvents for use in NMR experiments were dried as their protiated analogues but were vacuum transferred from the drying agent.

$Ru(\eta^2\text{-}CH_2PMe_2)(Me)(PMe_3)_3$.

$Ru(PMe_3)_4(Me)_2$ [6] (1.12 g, 2.57 mmol) was dissolved in 100 ml of hexane in a closed glass vessel of 1 l volume to accommodate the methane produced by the reaction. The solution was degassed and heated to 150 °C for 20 h, over which time the solution turned dark brown. The solvent was removed and the residue was sublimed (85 °C, 10^{-3} Torr) to yield 435 mg (40.3%) of a slightly pink solid. MS (EI): 420 (M^+), 405 ($M - Me^+$), 344 ($M - PMe_3^+$). Anal. Calcd. for $C_{13}H_{38}P_4Ru$: C, 37.22; H, 9.13. Found: C, 37.19; H, 9.32.

$(PMe_3)_4Ru(OC_6H_4Me)_2$ (1)

To a stirring solution of $(PMe_3)_4Ru(Me)_2$ (82.4 mg, 0.189 mmol) in 10 ml of toluene, 2.2 equiv. of *p*-methylphenol (49.2 mg) in 1 ml of toluene was added by pipette at room temperature in the drybox. Evolution of gas was observed over a period of 2 h and the solution turned orange. After a period of 8 h, blocks of **1** crystallized from the reaction solution. The supernatant was decanted and then layered with 5 ml pentane and cooled to −40 °C for 8 h to yield 66.2 mg (56.8%) of **1** as yellow blocks. For microanalysis and kinetic studies, a portion of this material was recyrstallized by vapor diffusion of pentane into a solution of **1** in toluene. IR

(KBr) 3064 (m), 3042 (m), 3001 (m), 2974 (s), 2909 (s), 2854 (m), 1602 (s), 1547 (m), 1504 (s), 1494 (s), 1327 (s), 1303 (s), 1294 (s), 1277 (s), 1161 (m), 971 (s), 942 (s). Anal. Calcd. for $C_{28}H_{50}O_2P_4Ru$: C, 50.40; H, 8.13. Found: C, 50.55; H, 8.17.

$(PMe_3)_4Ru(\eta^2\text{-}OC_6H_3Me)$ (2)

To a stirred solution of $(PMe_3)_4Ru(\eta^2\text{-}PMe_2CH_2)(Me)$ (421 mg, 1.00 mmol) in toluene (15 ml), one equivalent of *p*-methylphenol (108 mg) in 1 ml toluene was added dropwise by pipette at room temperature. The clear solution turned yellow/orange upon addition of the phenol. The solution was then transferred to a sealed glass reaction vessel, degassed and heated to 85 °C for 3 h. After this time the reaction was allowed to cool to room temperature at which point pale yellow blocks of **2** crystallized from the reaction mixture. The supernatant was decanted and then layered with 5 ml pentane followed by cooling to −40 °C to provide 322 mg of **2** (61% total yield) as yellow blocks. IR: 3029 (m), 2968 (m), 2902 (s), 2852 (m), 1439 (s), 1426 (m), 1297 (m), 1280 (m), 1250 (m), 1231 (m), 1219 (m), 1190 (m), 970 (m), 941 9s), 857 (m), 712 (m), 665 (m), 542 (m). Anal. Calc. for C_{19} $H_{42}OP_5Ru$: C, 44.61; H, 8.28. Found: C, 44.80; H, 8.41.

$(PMe_3)_3(\eta^2\text{-}PMe_2OC_6H_3)Ru(OC_6H_4Me)$ (3)

A solution of 120 mg (0.194 mmol) of **1** in toluene (70 ml) was heated for 8 h at 100 °C in an evacuated, sealed glass vessel. No significant color change occurred in the initial yellow solution. After this time the solvent was removed under reduced pressure. The resulting solid was dissolved in a minimum amount of toluene (1.5 ml), and vapor diffusion of pentane into the toluene solution at room temperature for 24 h yielded 40.8 mg (34.0%) of **3** as yellow blocks. IR: 2996, (m), 2988 (m), 2969 (m), 2958 (m), 2907 (m), 1601 (m), 1409 (s), 1498 (s), 1441 (m), 1323 (s), 1303 (m), 1293 (m), 1282 (m), 1180 (m), 946 (s), 935 (s), 933 (s), 858 (s), 816 (s), 716 (s): anal. Calcd. for $C_{25}H_{46}O_2P_4Ru$: C, 49.67; H, 7.67. Found: C, 49.87; H, 7.43.

Crystal and molecular structure determination of 3

Pale, clear yellow plate-like crystals of the compound were obtained by slow cooling to −30 °C from pentane/toluene. Fragments cleaved from some of these crystals were mounted on glass fibers using polycyanoacrylate cement. The X-ray structure determination was carried out by Dr F.J. Hollander of the UC Berkeley X-ray Diffraction Facility (CHEXRAY). Preliminary precession photographs indicated monoclinic Laue symmetry and yielded approximate cell dimensions.

The crystal used for data collection was then transferred to our Enraf-Nonius CAD-4 diffractometer [16] and centered in the beam. Automatic peak search and indexing procedures yielded the monoclinic reduced primitive cell. The final cell parameters and specific data collection parameters for this data set are given in Table 4. Due to some errors on set-up, the data collection parameters were not ideal, and a significant number of data suffered from overlap of neighboring data.

The 8048 raw intensity data were converted to structure factor amplitudes and their esd's by correction for scan speed, background and Lorentz and polarization effects. Inspection of the intensity standards revealed a variation of ±1.5 % of the original intensity. No correction for crystal decomposition was necessary. Inspection of the azimuthal scan data showed a variation $I_{min}/I_{max} = 0.91$ for the average curve. An empirical correction based on the observed variation was applied to the

data ($T_{max} = 1.0$, $T_{min} = 0.91$). Removal of systematically absent data left 7877 unique data in the final data set. Further rejection of a rough cone of data which showed themselves to be severely affected by overlap left a final total of 7642 acceptable data.

The structure was solved by Patterson methods and refined via standard least-squares and Fourier techniques. Following refinement of all atoms with anisotropic thermal parameters, data suffering from extreme overlap were removed from the data set as noted above. However, it is certain that other data suffer likewise, but were simply not obvious. In a final difference Fourier map peaks were found corresponding to the positions of only a few of the expected hydrogen atoms. No hydrogens were included in the calculation of structure factors for the last cycles of least squares.

The final residuals for 557 variables refined against the 5406 data for which $F^2 > 3\sigma(F^2)$ were $R = 5.93\%$, $R_w = 7.75\%$, and GOF = 3.00. The R value for all 1392 data points was 13.2%.

The quantity minimized by the least squares program was $\Sigma w(|F_o| - |F_c|)^2$ where w is the weight of intense reflections, was set to 0.03 throughout the refinement. The analytical forms of the scattering factor tables for the neutral atoms were used and all scattering factors were corrected for both the real and imaginary components of anomalous dispersion.

Inspection of the residuals ordered in ranges of $\sin(\theta)/\lambda$, $|F_o|$, and parity and value of the individual indexes showed no features or trends not previously noted. The largest peak in the final difference Fourier map had an electron density of 0.76 $e^-/Å^3$ and the lowest excursion -0.61 $e^-/Å^3$. There was no indication of secondary extinction in the high-intensity low angle data.

Kinetic analysis

Two stock solutions were prepared. Into a 3 ml volumetric flask was weighed 14.7 mg (0.0287 mmol) of **3** and 3.1 mg (0.0287) of *p*-cresol, followed by addition of toluene-d_8 to give a 0.00957 *M* solution of both reagents. Into a 2 ml volumetric flask was weighed 11.9 mg of **1** (0.0193 mmol) followed by addition to toluene to give a 0.00964 *M* solution. To one 9 in. NMR tube was added 0.70 ml of the solution of **1**, to another tube was added 0.70 ml of the solution of **1** and *p*-methylphenol, and to a third tube was added 0.40 ml of the solution of **1** and 0.30 ml of the solution of **3** and *p*-cresol. To each tube was added 2–3 mg ferrocene as an internal standard. Each tube was freeze pump thawed through three cycles and sealed to give a tubes of equal length. The tubes were heated at 65°C in a factory-calibrated Neslab Exocal Model 251 constant-temperature bath filled with Dow Corning 200 silicone fluid, and cooled in a room temperature water bath after removal from the 65°C bath. All three reactions were monitored to 2.5 half-lives by ambient-temperature ^1H NMR spectrometry by integrating the methyl protons of the *p*-methylphenol group vs. the ferrocene internal standard. An infinity point was obtained experimentally by heating the three tubes to 85 for 8 h and obtaining ^1H NMR spectra after this time. All spectra were taken with a single acquisition and double checked with a second acquisition after a delay of at least $10T_1$. All three kinetic plots displayed excellent linearity with correlation coefficients of 0.985 or better, and the yield of each reaction was greater than 98%.

Dependence of reaction on PMe_3 concentration

Four NMR tubes were prepared. Two were prepared exactly as the tubes described in the kinetic analysis section containing only **1**, except that 10 equiv. (0.0675 mmol) PMe_3 was added to one of these tubes to give a concentration of 0.0964 *M* PMe_3. Two other tubes were prepared in the same manner except the solution of **3** and *p*-cresol was used instead of the solution of **1**. The tubes were heated to 65 °C for 3 d and monitored periodically by ^1H and ^{31}P NMR spectrometry. The addition of PMe_3 had no effect on the rate at which equilibrium was established. However, no product was observed after 3 d at for the tubes containing added PMe_3, while reaction was complete for the samples containing no additional PMe_3.

Acknowledgements

We thank Dr. Thomas H. Tulip for providing us with crystallographic details on the structure of $(PMe_3)_4Ru(\eta^2\text{-}CH_2C_6H_4)$. This work was supported by the National Institutes of Health (Grant no. GM-25459). The crystal analysis was performed by Dr F.J. Hollander, staff crystallographer at the UC Berkeley X-ray crystallographic facility (CHEXRAY).

References and notes

1 S.A. McAuliffe, Transition Metal Complexes of Phosphorus, Arsenic and Antimony Ligands, Wiley, New York, 1973; C.A. McAuliffe and W. Levason, Phosphine, Arsine, and Stibine Complexes of the Transition Elements, Elsevier, Amsterdam, 1979.

2 (a) C.A. Tolman, Chem. Rev., 77 (1977) 313; (b) Md. M. Rahman, L. Hong-Ye, K. Eriks, A. Prock and W.P. Giering, Organometallics, 8 (1989) 1.

3 (a) R.H. Crabtree, Chem. Rev., (185) 245; (b) P.J. Derosiers, R.S. Shinomoto and T.C. Flood, J. Am. Chem. Soc., 108 (1986) 7964.

4 (a) P.E. Garrou, Chem. Rev., 85 (1985) 171; (b) N.M. Doherty, G. Hogarth, S.A.R. Knox, K.S. Macpherson, F. Melchior and A.G. Orpen, J. Chem. Soc., Chem. Commun., (1986) 540. (c) G.R. Doel, N.D. Feasey, S.A.R. Knox, A.G. Orpen and J.J. Webster, Chem. Soc., Chem. Commun., (1986) 542; (d) H. Benlaarab, B. Chaudret, F. Dahan and R.J. Poilblanc, Organomet. Chem., 320 (1987) C51. (e) W.D. McGhee, T. Foo, F.J. Hollander and R.G. Bergman, J. Am. Chem. Soc., 110 (1988) 8543.

5 (a) A. Gillie and J.K. Stille, J. Am. Chem. Soc., 102 (1980) 4933. (b) K. Kikukawa, T. Yamane, Y. Ohibe, M. Takagi and T. Matsuda, Bull. Chem. Soc. Jpn., 52 (1979) 1187. (c) K. Kikukawa, M. Takage and T. Matsuda, Bull. Chem. Soc. Jpn., 52 (1979) 1493. (d) J.V. Ortiz, Z. Havlas and R. Hoffmann, Helv. Chim. Acta, 67 (1984) 1.

6 R.A. Andersen, R.A. Jones and G. Wilkinson, J. Chem. Soc., Dalton Trans., (1978) 446.

7 (a) W.K. Wong, K.W. Chiu, J.A. Slatter, G. Wilkinson, M. Motevalli and M.B. Hursthouse, Polyhedron, 3 (1984) 1255; (b) J.A. Slatter, G. Wilkinson, M. Thornton-Pett and M.B. Hursthouse, J. Chem. Soc., Dalton Trans., (1984) 1255. (c) J.C. Calabrese, M.C. Colton, T. Herskovits, U. Klabunde, G.W. Parshall, D.L. Thom and T.H. Tulip, Ann. N.Y. Acad. Sci., 415 (1983) 302; 9d) M. Antberg, L. Dahlenburg, K.M. Frosin and N. Höck, Chem. Ber., 121 (1988) 859. (e) L. Dahlenburg and K.M. Frosin, Chem. Ber., 121 (1988) 864. (f) J.F. Hartwig, R.A. Andersen and R.G. Bergman, J. Am. Chem. Soc., 11 (1989) 2717.

8 (a) J.F. Nixon and A. Pidcock, Ann. Rev. NMR Spectrosc., 2 (1969) 345; 9b) J.M. Verkade and L.D. Quin (Eds.) Phosphorus-31 NMR Spectroscopy in Stereochemical Analysis, VCH Publishers, New York, 1987.

9 (a) W.J. Sime and T.A. Stephenson, J. Chem. Soc., Dalton Trans., (1978) 1647; (b) ref. 7b p. 500.

10 An ORTEP is provided in ref. 7c, but no bond distances are given. The Ru–P bond lengths are 2.343(1), 2.347(1), (mutually *trans* PMe_3 groups) 2.321(1), 2.321(1) (mutually *cis* PMe_3 groups), personal communication.

11 H.J. Plastas, J.M. Stewart and S.O. Grim, J. Am. Chem. Soc., 91 (1969) 4326.
12 M.J. Kruger, R.O. Heckroodt, R.H. Reimann and E.J. Singleton, Organomet. Chem., 87 (1975) 323.
13 H. Vahrenkamp, Chem. Ber., 104 (1971) 449.
14 M.J. Workulich, J.L. Atwood, L. Canada and J.D. Atwood, Organometallics, 4 (1985) 867.
15 R.G. Bergman, J.M. Buchanan, W.D. McGhee, R.A. Periana, P.F. Seidler, M.K. Trost and T.T. Wenzel, in: A.L. Wayda and M.Y. Darensbourg (Eds.), Experimental Organometallic Chemistry: A Practicum in Synthesis and Characterization, ACS Symposium Series 357, American Chemical Society, Washington, DC, 1987, p. 227.
16 For a description of the X-ray diffraction and analysis protocols used, see (a) W.H. Hersh, F.J. Hollander and R.G. Bergman, J. Am. Chem. Soc., 105 (1983) 5834; 9b) R.B. Roof Jr., A Theoretical Extension of the Reduced-Cell Concept in Crystallography, Publication LA-4038, Los Alamos Scientific Laboratory, Los Alamos, NM, 1969; (c) D.T. Cromer and J.T. Waber, International Tables for X-ray Crystallography, Kynoch Press, Birmingham, England, 1974, Vol. IV, Table 2.2B.